Advances in Aircraft and Spacecraft Science, *Vol. 3, No. 2 (2016) 211-224*
DOI: http://dx.doi.org/10.12989/aas.2016.3.2.211

Nonlinear model based particle swarm optimization of PID shimmy damping control

Andrea Alaimo[1a], Alberto Milazzo[*2] and Calogero Orlando[1b]

[1]*Università di Enna "Kore", Cittadella Universitaria 94100, Enna, Italy*
[2]*Università di Palermo, Viale delle Scienze Ed. 8, 90128 Palermo, Italy*

(Received August 22, 2015, Revised November 14, 2015, Accepted November 28, 2015)

Abstract. The present study aims to investigate the shimmy stability behavior of a single wheeled nose landing gear system. The system is supposed to be equipped with an electromechanical actuator capable to control the shimmy vibrations. A Proportional-Integrative-Derivative (PID) controller, tuned by using the Particle Swarm Optimization (PSO) procedure, is here proposed to actively damp the shimmy vibration. Time-history results for some test cases are reported and commented. Stochastic analysis is last presented to assess the robustness of the control system.

Keywords: nose landing gear; shimmy vibration; active control

1. Introduction

Shimmy vibration is a phenomenon that regards dynamics of steerable wheels and, thus, it is of relevant aeronautical interest for landing gear dynamics and for motorcycles or cars tire dynamics, Besselink (2000), Pacejka (2005). During the rolling motion, the wheel can oscillate about the steering axis as consequence of the tire-road interaction and of the torsional stiffness and damping characteristic of the landing gear strut, Stépán (2002). The interplay of the tire-road dynamics and of the torsional elastic behavior of the gear strut are such that the shimmy oscillations can be classified as a self-sustained and inherently non-linear phenomenon, Howcroft *et al*. (2014). Moreover, the complexity of the shimmy behavior deeply increases when the influences of other factors are taken into account, namely the gear strut lateral and vertical dynamics, Thota (2009), the non-linearity introduced by the torque link torsional play, Sateesh and Maiti (2009), and the delay effect introduced by the tire elasticity, Takács *et al*. (2009).

Despite of the causes, it is known that shimmy vibrations of landing gears can increase in amplitude and frequency at high rate and can cause severe damages to the aircraft before the pilot can counteract it, Moreland (1954). For this reason, it is important to equip any landing gear that is prone to the shimmy phenomenon with damping systems. Generally, by increasing the torsional stiffness of the gear strut the shimmy vibrations are reduced in amplitude. However, it is common

∗Corresponding author, Professor, E-mail: alberto.milazzo@unipa.it
[a]Professor, E-mail: andrea.alaimo@unikore.it
[b]Ph.D., E-mail: calogero.orlando@unikore.it

http://www.techno-press.org/?journal=aas&subpage=7 ISSN: 2287-528X (Print), 2287-5271 (Online)

to install a small shock absorber between the nose wheel fork and the nose wheel cylinder to passively dampen shimmy vibrations. A drawback of passive hydraulic shimmy dampers is their need to be periodically inspected for leaks and kept fully operational by adding fluid to capacity, EASA and TTS (2010). Rubber-piston shimmy dampers can be employed; indeed, they are certified for some aircrafts and they exhibit a long service life without the necessity to replenish fluid, FAA-H-8083-312(2012). Independently from the kind of shimmy dampers, their passive behavior allows optimal performances only in the design conditions. Any variation of the loading conditions, of the tire-road interaction or of the gear leg structural properties can drastically reduces the damping authority of system that can also become instable, Huynh *et al*. (2008). In order to increase the robustness of the shimmy damping system, both semi-active and active control approaches have been investigated. Among others, a semiactive shimmy damper based on magnetorehological (MR) fluid has been proposed and numerically analyzed by Atabay and Ozkol (2014) proving that the MR shimmy damper added to the system allows to dampen shimmy vibration even in presence of torsional play and very low hydraulic damping constant using about one Ampere current input. On the other hand, active approaches based on both state-feedback and output-feedback fuzzy control have been proposed and studied (Pouly *et al*. 2008, 2011) evidencing the feasibility of active shimmy vibration suppression. No matter of the control solutions proposed or adopted in the literature, the shimmy vibration of the Nose Landing Gear (NLG) is still an open problem from both the theoretical and technological point of view, Bonfè (2011).

In this paper, an electromechanical actuator based PID control scheme is used to damp the shimmy vibration of a NLG. Despite the great variety of advanced control schemes proposed and validated, the PID algorithm is still one of the most used because of its simplicity, Ang *et al*. (2005). Its tuning represents the bottleneck of the method since no standardized procedure exists to set the involved parameters, Ang *et al*. (2005). Here, a particle swarm optimization (PSO) procedure, Shi and Eberhart (1999), is implemented to obtain the optimal selection of the PID parameter based on a non-linear NLG model, which takes the actuator dynamics into account, Somieski (1997), Pouley *et al*. (2011). The aim of the paper and its contribution to the field is to numerically demonstrate the feasibility and the stochastic robustness of an active PID shimmy controller based on the use of a electromechanical actuator. The equations of motion of the controlled landing gear shimmy are given in Section 2 along with the particle swarm optimization scheme used to select the PID parameters. Section 3 reports the model validation results and the convergence analyses of the PSO procedure as well as time-history results for some selected test cases and a probabilistic robustness study. Eventually, conclusions are given in Section 4.

2. PSO-PID shimmy damping control

The system under consideration is schematically shown in Fig. 1. It consists of a turning tube and a sliding tube connected by the torque link to ensure the torsional stiffness of the gear strut and a caster fork that links the single wheel to the sliding tube. This scheme is a simplification of an aircraft nose landing gear already proposed by Somieski (1997) and successively extended by Pouly *et al*. (2001) to take into account the presence of an electromechanical actuator, which is assumed capable of applying the requested control torque to the turning tube. The problem governing equations are given first in the next subsection and then the PID control scheme is presented along with the particle swarm optimization algorithm used for the selection of the PID

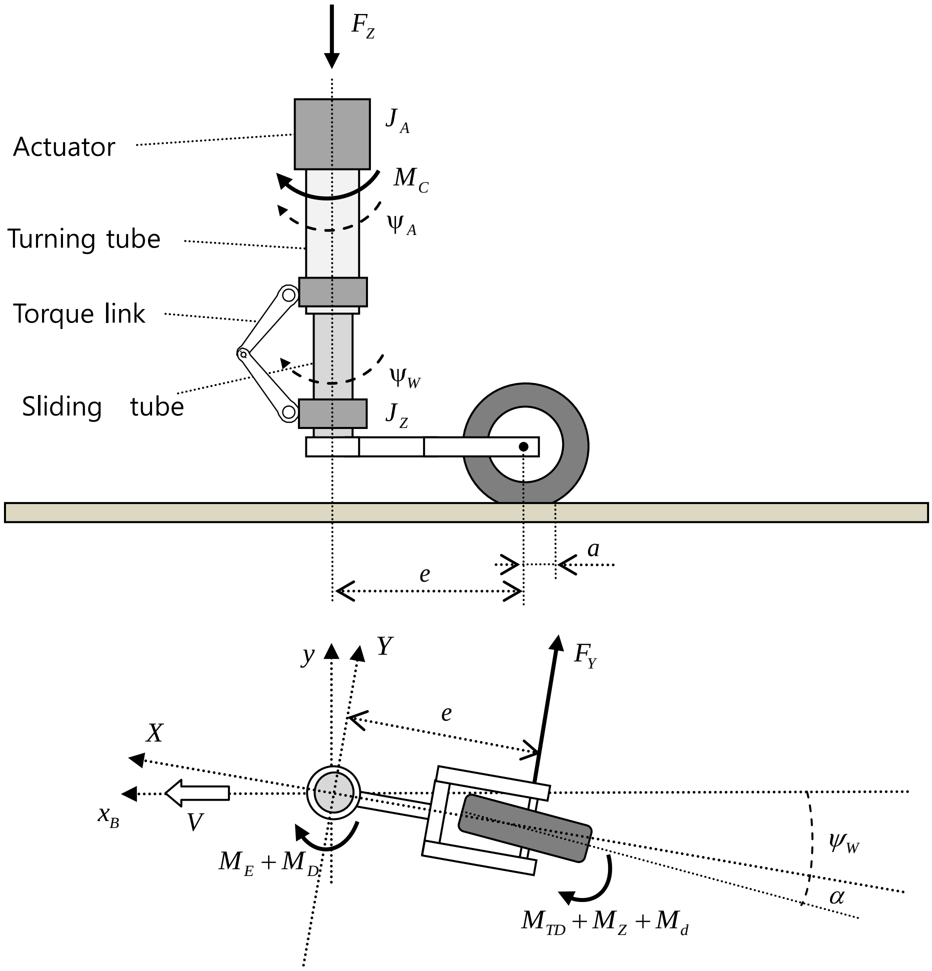

Fig. 1 Model of the nose landing gear

parameters.

2.1 Nonlinear shimmy model

With reference to Fig. 1, let J_Z and e be the mass moment of inertia about the vertical steering axis and the caster length, respectively, and let J_A denote the electromechanical actuator mass moment of inertia. The NLG is moving with velocity V along the x_B direction. The variables used to describe the kinematics of the NLG about the vertical steering axis are the rotation angle of the caster fork ψ_W, the yaw angle of the turning tube ψ_A and the sideslip angle of the tire α.

The problem governing equations are obtained from the torsional dynamics of both the NLG and the actuator and from a simplified model of the lateral tire-road interactions. Firstly, the torsional dynamic equation of the actuator is written and it reads as

$$J_Z \ddot{\psi}_A = -M_E - M_D - K_{DA} \dot{\psi}_A + M_C \tag{1}$$

where $M_E=K_S(\psi_A-\psi_W)$ is the linear spring torque provided by the scissor link, $M_D = K_D(\dot{\psi}_A - \dot{\psi}_W)$ is the damping torque provided by the shimmy damper and the viscous friction in the bearings of the NLG shock absorber, M_C is the control torque commanded by the actuator, K_S is the NLG torsional stiffness whereas K_D and K_{DA} are the NLG and the actuator damping constants, respectively. Secondly, the equilibrium equation for the NLG is written as

$$J_Z\ddot{\psi}_W = M_E + M_D + M_Z - eF_Y + M_{TD} + M_d \tag{2}$$

where M_d is the external torque disturbance applied to the tire, M_Z is the so-called self-aligning moment caused by the tire lateral elastic deflection about the center of the tire, F_Y is the tire lateral force. In Eq. (2), M_{TD} is the damping moment provided by the tire deflection that reads as

$$M_{TD} = \frac{\kappa}{V}\dot{\psi}_W \tag{3}$$

where κ is the constant of tread width tire moment. More particularly, the introduced tire quantities are defined as

$$F_Y = \begin{cases} c_{F\alpha}\alpha F_z & |\alpha| \le \delta_F \\ c_{F\alpha}\delta_F F_z sign(\alpha) & |\alpha| > \delta_F \end{cases} \tag{4}$$

$$M_Z = \begin{cases} c_{M\alpha}\dfrac{\delta_M}{\pi}F_z \sin\left(\dfrac{\pi}{\delta_M}\alpha\right) & |\alpha| \le \delta_M \\ 0 & |\alpha| > \delta_M \end{cases} \tag{5}$$

where $c_{F\alpha}$ and $c_{M\alpha}$ are the force and moment derivatives with respect to α while δ_F and δ_M are the limiting angles for the tire force and moment, respectively. As it appears from Eqs. (4) and (5), both F_Y and M_Z are functions of the side slip angle α and of the ground normal reaction F_Z; they represent a simple, but still realistic nonlinear model of the lateral force and self aligning torque generated by the tire in contact with the road, Somieski (1997).

Lastly, the governing equation for the lateral dynamics of the tire is considered. It is written in terms of the sideslip angle by using the elastic string model, Pacejka (2005)

$$\dot{\alpha} + \frac{V}{\sigma}\alpha = \frac{V}{\sigma}\psi_W + \frac{e-a}{\sigma}\dot{\psi}_W \tag{6}$$

being $\sigma=3a$ the relaxation length of tire deflection and a the half contact length of the tire and the ground, see Besselink (2000) and Pacejka (2005). In writing Eq. (6) the approximation $y_T \approx \alpha\sigma$ has been used, being y_T the tire lateral deflection.

2.2 PSO-PID control

A Proportional Integral Derivative controller is proposed to lead the actuator in such a way the error function $\varepsilon(t)=\psi_{W,d}(t)-\psi_W(t)$, being $\psi_{W,d}$ the desired value of the controlled variable, is minimized and the nose landing gear shimmy vibrations are actively dampened. The control torque provided by the actuator is thus the sum of a term proportional to the current error, plus a term proportional to the integral of the error signal, plus a term proportional to the error time derivative, and writes as

$$M_C(t) = K_P \varepsilon(t) + K_I \int_0^t \varepsilon(\tau) d\tau + \frac{K_D}{\tau_{DF}} \varepsilon_D(t) \tag{7}$$

where K_P, K_I and K_D are the proportional, integral and derivative gains. In Eq. (7) τ_{DF} is the constant of the time derivative filter used to smooth noise effects on the measured error signal. In particular, the filtered value of the error derivative considered in the PID scheme given in Eq. (7), namely ε_D, is governed by the following first order differential equation

$$\tau_{DF} \dot{\varepsilon}_D + \varepsilon_D = \dot{\varepsilon} \tag{8}$$

With the aim of tuning the parameters of the PID controller, namely K_P, K_I, K_D and τ_{DF}, the particle swarm optimization technique is adopted. The PSO is a stochastic optimization technique based on simplified social model. Each particle has a number of qualities, associated with the problem solution, that allow to locate the *i-th* particle in the problem space by means of an *n-dimensional* vector, the so called position variables p^i. For the problem under consideration, the position variables vector particularizes as $p^i = [\, K_P \;\; K_I \;\; K_D \;\; \tau_{DF} \,]$. At first, the swarm is initialized randomly and then, at the successive steps, it is updated as

$$p^i_{\lambda+1} = p^i_\lambda + dp^i_{\lambda+1} \tag{9}$$

In Eq. (9), λ is the iteration step, $dp^i_{\lambda+1}$ is the particle velocity computed on a unitary step increment according to Shi and Eberhart (1999) as

$$dp^i_{\lambda+1} = \mu dp^i_\lambda + c_c r_1 \left(p^i_b - p^i_\lambda \right) + c_s r_2 \left(p^g_b - p^i_\lambda \right) \tag{10}$$

where μ is the inertia weight, c_c and c_s are acceleration coefficients, called cognitive and social constant, respectively, r_1 and r_2 are coefficients chosen randomly in the interval [0, 1]. p^i_b is the personal best position of the *i*-th particle, i.e. the position that gives the best fitness value with respect to the chosen objective function, while p^g_b is the global best position of the entire swarm. Moreover, in order to balance the exploration and the exploitation processes of swarm, the linear variation of the inertia weight is taken into account as

$$\mu = \mu_{Max} \left(1 - \frac{\lambda}{\lambda_{Max}} \right) + \mu_{\min} \frac{\lambda}{\lambda_{Max}} \tag{11}$$

where μ_{min} and μ_{Max} are the minimum and maximum value of the inertia weight while λ_{Max} is the maximum number of iterations. In this paper, the objective function considered in running the PSO procedure for the active shimmy vibration suppression is the integral of square error, namely

$$\Im = \int_0^{T_W} \varepsilon^2 dt \tag{12}$$

where T_W is the time window extent over which the fitness value is computed.

3. Results

Table 1 Model data

Parameter	Value	Parameter	Value
Forward velocity	V=80 [m/s]	Half contact length	a=0.1 [m]
Inertia of actuator	J_a=0.1 [kg m^2]	Caster length	e=0.1 [m]
Inertia of NLG	J_z=1 [kg m^2]	Cornering stiffness	$c_{F\alpha}$=20 [rad^{-1}]
Actuator damping	B_a=0.1 [Nms/rad]	Self-aligning stiffness	$c_{M\alpha}$=−2 [rad^{-1}]
Vertical load	F_z=9 [kN]	Limiting angle for lateral force	δ_F=5 [deg]
Stiffness constant	K_S=100 [kNm/rad]	Limiting angle for self-aligning moment	δ_M=10 [deg]
Damping constant	K_D=10 [Nsm/rad]	Constant of tread width tire moment	κ=−270 [Nm^2/rad]

The proposed PSO-PID controller for the active suppression of the NLG shimmy vibration was analyzed numerically. The model parameters of the investigated NLG were taken from literature, see Somieski (1997) and Pouley *et al*. (2011), and they are collected in Table 1.

To check the present results with those by Pouley *et al*. (2011), three different case studies were solved. These are described in the next section along with the model validation under open loop condition. For all of the case studies, the desired value of the caster-fork rotation angle was $\psi_{W,d}$=0 deg while the maximum allowed value of the wheel rotation angle was $\psi_{W,\mathrm{Max}}$=1.5 deg. It was also requested that the settling time of the shimmy vibration phenomenon is no longer than $t_{S,\mathrm{Max}}$=0.2 s and maximum value of the torque exerted by the actuator should not exceed $M_{C,\mathrm{Max}}$=2 kNm. Results from the PSO-PID tuning procedure and from closed loop control simulations are given and commented in section 3.2. Last, the controller robustness was verified using the stochastic robustness analysis in section 3.3.

3.1 Case studies and model validation

Three different case studies were taken into account that are of interest from the aeronautical point of view, namely *Case 1:* tire damage, *Case 2:* rough runaway and *Case 3:* rough runaway under increasing velocity. In both the tire damage and rough runaway case studies, the forward velocity of the aircraft was set to V=80 m/s, as shown in Table 1. In the former case an external torque disturbance pulse of amplitude M_d=1 kNm was applied to the tire for 0.1 *s* while, for carrying out simulations in the latter case, a random torque disturbance characterized by zero mean value and standard deviation SD(Md)=0.1 kNm was considered. Open loop results for both Cases 1 and 2 are reported in terms of caster-fork rotation angle history in Fig. 2 and Fig. 3, respectively, where the applied disturbances are also depicted. Fig. 2 shows that the shimmy phenomenon appears with the impulse disturbance in the tire damage case while under the rough runaway condition, see Fig. 3, the wheel starts to vibrate slowly. However, in both cases the amplitude of the rotation angle increases with time until it reaches a limit cycle of about 22.4 deg. These trends are confirmed by previously published work by Somieski (1997), Pouley *et al*. (2011).

Open loop results obtained under the rough runway and increasing speed condition are reported

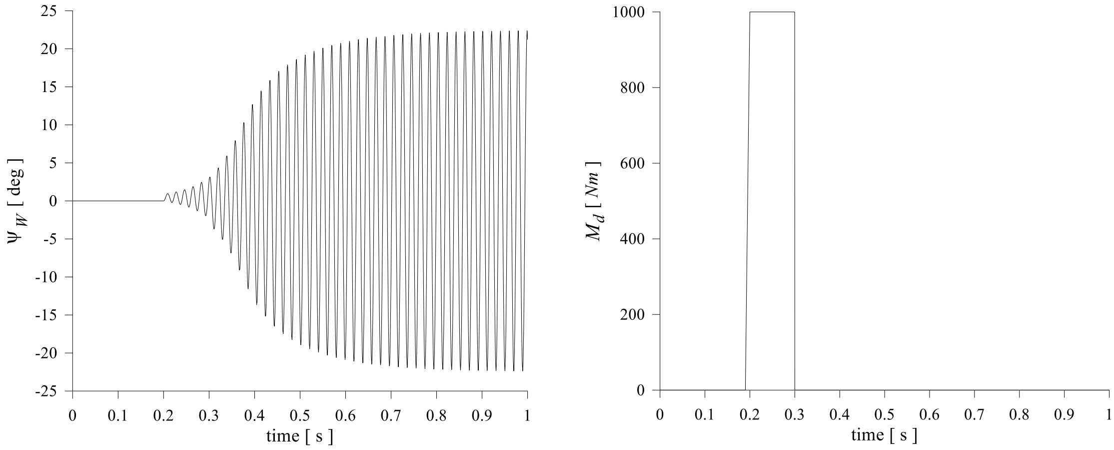

(a) time history of the rotation angle $\psi_W(t)$ (b) time history of the disturbance torque $M_d(t)$

Fig. 2 Tire damage case: open loop results

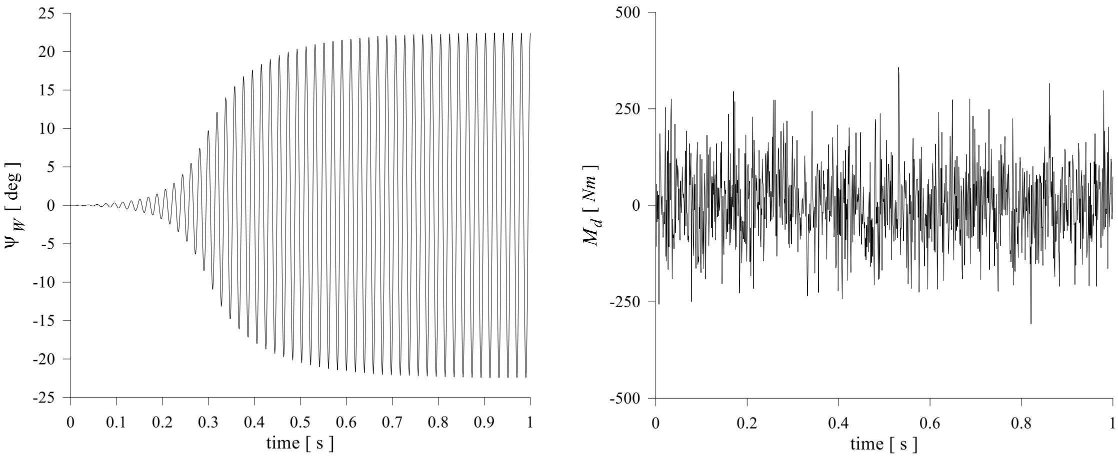

(a) time history of the rotation angle $\psi_W(t)$ (b) time history of the disturbance torque $M_d(t)$

Fig. 3 Rough runway case: open loop results

in Fig. 4 along with the time history of the aircraft forward velocity. It was assumed that the aircraft speed starts from the value of 10 m/s and reach a final constant value of 80 m/s with a constant acceleration of 5 m/s^2 that lasts for 14 s. The torque disturbance varied randomly with zero mean value and standard deviation SD(*Md*)=0.1 kNm.

The system behavior resulted stable during the first three seconds of analysis, when the aircraft forward velocity was V<25 m/s, then the shimmy vibration increased rapidly to about 26 deg approaching the limit cycle value. This behavior confirmed that the critical forward velocity of the analyzed NLG system, i.e. the velocity above which shimmy may occur, is 25 m/s and the shimmy frequency is of 51 Hz. These results match well literature data, Somieski (1997), Pouley *et al*. (2011). Open loop results for the three analyzed study cases are summarized in Table 2 in terms of maximum absolute value of the rotation angle ψ_W and in terms of the objective function value, namely Eq. (12) computed over 15 seconds of analysis.

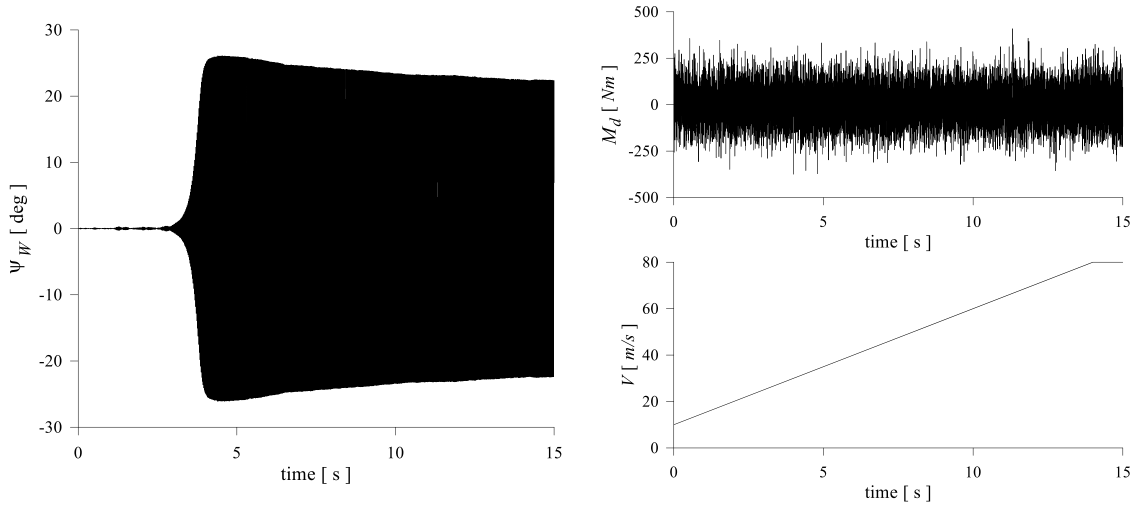

(a) time history of the rotation angle $\psi_W(t)$ (b) disturbance torque $M_d(t)$and velocity history

Fig. 4 Increasing velocity case: open loop results

Table 2 Open loop results

Cases	$\lvert\psi_W\rvert_{Max}$ [deg]	$\Im$ [rad^2 s]
Tire Damage	22.4	1.1099
Rough Runaway	22.4	1.1117
Increasing Velocity	26.0	0.9894

3.2 PSO-PID control analysis

In order to design the PID active shimmy controller using the PSO technique the first case study, namely the tire damage one, has been considered. The objective function to be minimized was computed over 1 second of analysis. A trial and error procedure has been used to set the parameters for the PSO problem by using the following procedure parameters. The number of particles is 20; the cognitive and social constants, c_c and c_s, were set to 2.05; the minimum and maximum values of the inertia weight were μ_{min}=0.4 and μ_{max}=0.9 while the maximum number of iteration was set to 20. To take into account the probabilistic nature of the employed optimization algorithm, about 500 simulations have been run in order to gain a stochastically significant result. Fig. 5 shows the trend of the objective function; only 10 runs are plotted for the sake of simplicity, which demonstrate that 20 iterations are enough to ensure the minimum value of the objective function is reached ($\Im = 0.0218$ deg^2 s). The problem solution p^{best}, that represents the PSO optimal selection of PID parameters, resulted as K_P=872.5 Nm/deg, K_I=2.745 Nm/s deg, K_D=8.854 Nms/deg and τ_{DF}=3.5902 ms.

The closed loop time history of the caster-fork angle under the tire damage case is shown in Fig. 6 along with the control moment needed to damp the shimmy vibration. From Fig 6 (a) it appears that the shimmy vibration started with the pulse disturbance at the instant t=0.2 s and the maximum value of the rotation angle was $|\psi_W|_{\text{Max}}$=0.714 deg, then it rapidly decreased with settling time t_s=0.052 s when ψ_W<0.05 deg. The damping capability of the proposed PSO tuned

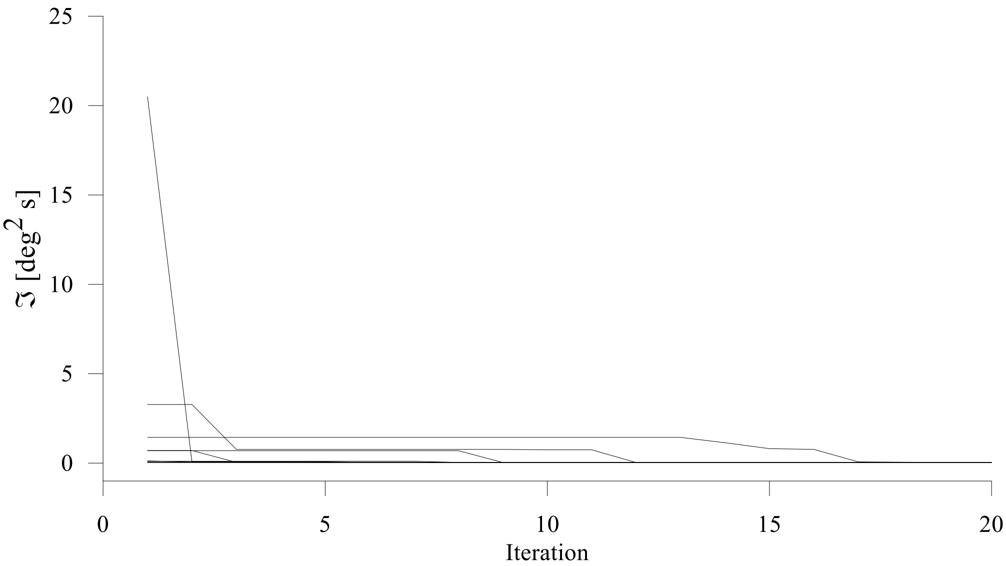

Fig. 5 PSO convergence results

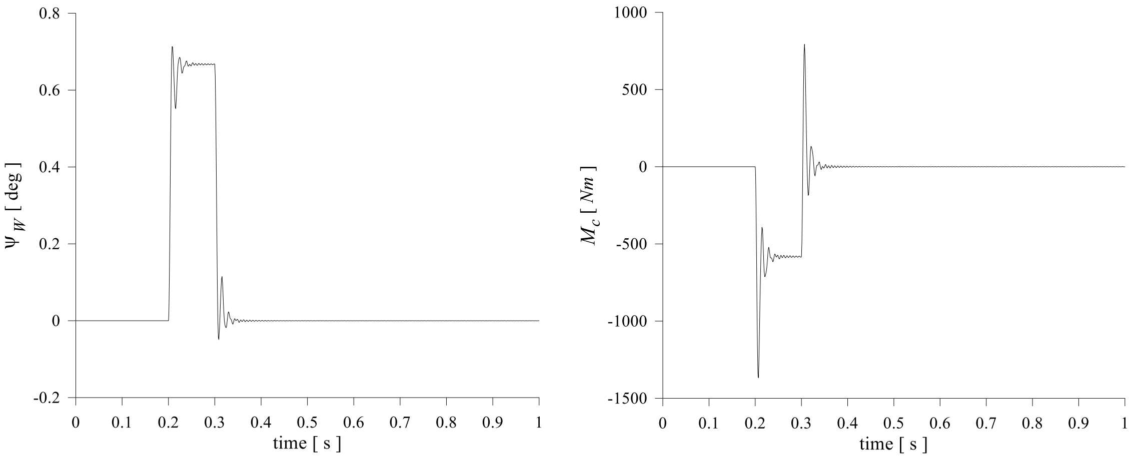

(a) time history of the rotation angle $\psi_W(t)$ (b) time history of the control torque $M_C(t)$

Fig. 6 Tire damage case: closed loop results

PID controller was assessed by computing the damping ratio to have an objective control criterion. To compare the present results with those by Pouly *et al*. (2011), the damping ratio was computed by using the values of two successive minima, ψ_{W1} and ψ_{W2} respectively, after the disappearance of the disturbance torque as

$$\varsigma = \frac{1}{\sqrt{1+\left(2\pi/\Delta\right)^2}} \tag{13}$$

where $\Delta=\log(\psi_{W1}/\psi_{W2})$. In particular, the values of the two successive minima were $\psi_{W1}=-0.04904$ deg and $\psi_{W2}=-0.01812$ deg, thus the damping ratio resulted as $\varsigma=0.1565$, which was in accordance

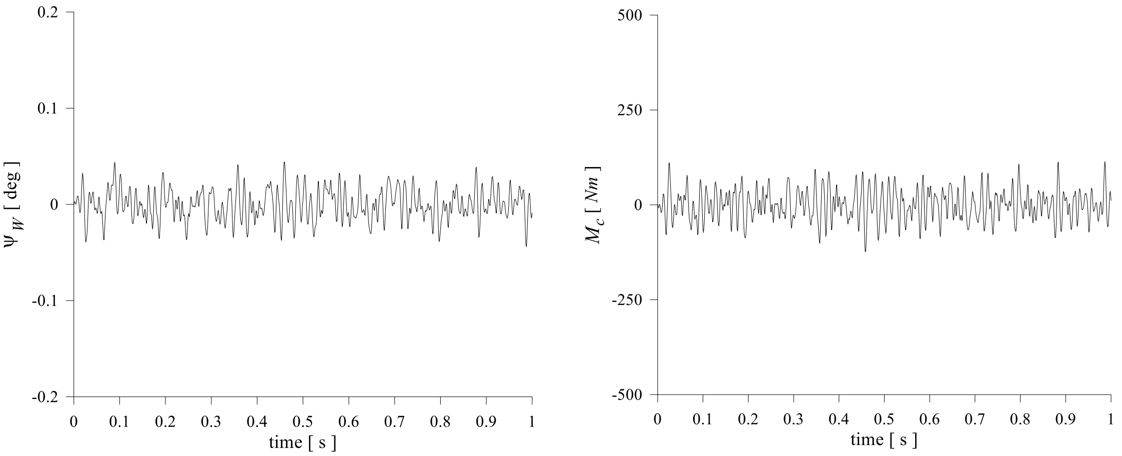

(a) time history of the rotation angle $\psi_W(t)$ (b) time history of the control torque $M_C(t)$

Fig. 7 rough runaway case: closed loop results

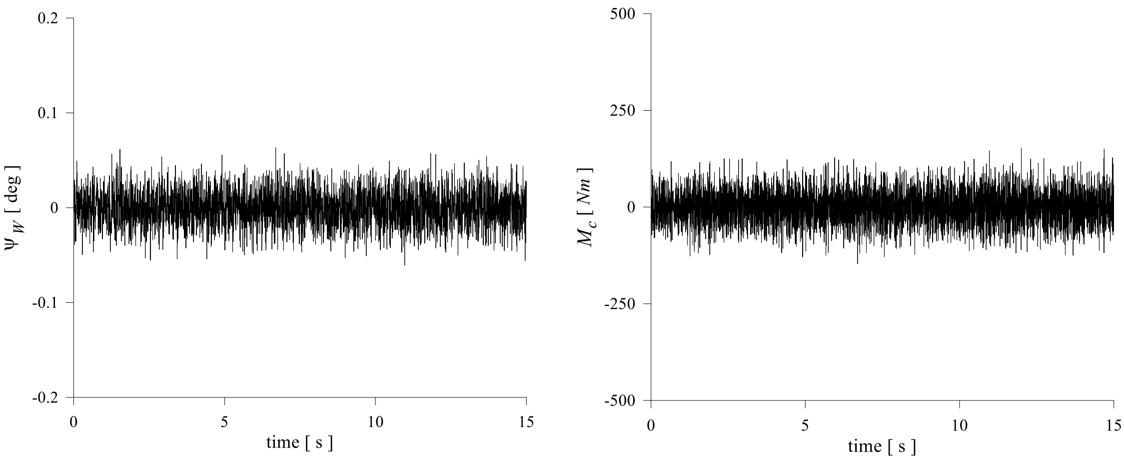

(a) time history of the rotation angle $\psi_W(t)$ (b) time history of the control torque $\psi_W(t)$

Fig. 8 Increasing forward velocity case: closed loop results

with the damping ratios obtained by Pouley *et al.* (2011) using both the direct and indirect fuzzy approaches. On the other hand, from Fig. 6(b) it appears that the maximum absolute value of the control torque was $|M_C|_{\text{Max}}$=1362 Nm which was less than the maximum allowed value $M_{C,\text{Max}}$..

The results with the PSO-PID active controller under the rough runaway condition are plotted in Fig. 7 in terms of nose wheel rotation angle and control torque exerted by the actuator. Despite of the random disturb at high velocity, which was such to engender limit cycle oscillation in the open loop case (see Fig. 3), the maximum absolute value of the shimmy oscillation amplitude did not exceed 0.05 deg while the maximum value of the control torque was 124 Nm. Such variations of the wheel angle are small and cannot cause damage to the system.

The last closed loop test case to be analyzed in comparison with the open loop one was the rough runaway with increasing forward velocity. The results are shown in Fig. 8 and allowed to verify that the active controller did not influence the system stability behavior below the critical

Table 3 Closed loop results

Cases	t_s [sec]	$\left\|\psi_W\right\|_{Max}$ [deg]	$\left\|M_C\right\|_{Max}$ [Nm]	$\Im$ [rad^2 s]
Tire Damage	0.052	0.714	1362	1.31e-05
Rough Runaway	0	0.045	124	1.33e-06
Increasing Velocity	14.95	0.063	152	1.32e-06

forward velocity of 25 m/s. Moreover, from Fig. 8 it appears that the active controller was capable of damping the shimmy vibration at high velocity.

Closed loop results for the three analyzed study cases are summarized in Table 3 in terms of maximum absolute value of the rotation angle ψ_W and in terms of the objective function value computed over 15 seconds of analysis. The maximum absolute value of the control torque $|M_C|_{\mathrm{Max}}$ is also reported along with the settling time t_S. In the rough runaway study case the settling time was zero since the absolute value of the caster-fork angle was less 0.05 deg over the 15 s of analysis. In the increasing velocity case, it could not be defined since the value of the wheel angle exceeded the limit value of 0.05 deg randomly, however it was always lower than 0.063 deg and thus it was not able to cause damage to the oscillating NLG wheel.

3.3 Sthocastic robusteness verification

Stochastic robustness analysis was used to estimate the damping capability of the proposed control system for the shimmy vibration problem, Ray and Stengel (1993). Mismatch between the actual and the nominal system are introduced by environment effects, systems failures, parameters estimation errors as well as by wear and manufacturing differences. This implies that a control system optimized for the nominal system may not be optimal for the actual one. Stochastic robustness analysis offers the possibility to investigate the robustness of the control system taking into account the probabilistic nature of uncertainties. Moreover, it also allows obtaining a controller, which is not over conservative neither insufficiently robust, Ray and Stangel (1992). The method is based on the definition of stability or performance criteria and on the Monte Carlo analysis of the probability $\hat{P}$ of violating such criteria. It follows that the stochastic robustness problem is binomial (the criterion under consideration is verified or not) and thus the confidence interval can be computed by the binomial test, Von Collani and Dräger (2001). In the present paper, four criteria were considered to investigate the robustness of the proposed PID control scheme, they write as

$$Criteria:\begin{cases} \left|\psi_w\right|_{Max} < \psi_{w,Max} \\ \left|M_C\right|_{Max} < M_{C,Max} \\ t_s < t_{s,Max} \\ \varsigma > \varsigma_{\min} \end{cases} \tag{14}$$

The minimum value of the damping ratio $\varsigma_{\min}$ used in Eq. (14) was selected from the work of Pouly *et al*. (2011) and specifies as $\varsigma_{\min}$=0.07. Each Monte Carlo evaluation was based on the solution of the problem governing equation taking into account the uncertainty of the problem parameters. More in detail, the variations of the stiffness K_S and the damping K_D constants are representative of wear or loose of tolerances; the uncertainties on cornering and self-aligning

Table 4 Probabilistic robustness data

Parameter	Value
Forward velocity	$V = \mathcal{U}\{25,80\}\ [m/s]$
Vertical load	$F_z = \mathcal{U}\{7.2,10.8\}\ [kN]$
Stiffness constant	$K_S = \mathcal{U}\{80,120\}\ [kN\,m/rad]$
Damping constant	$K_D = \mathcal{U}\{8,12\}\ [N\,s\,m/rad]$
Cornering stiffness	$c_{F\alpha} = \mathcal{U}\{16,24\}\ [rad^{-1}]$
Self-aligning stiffness	$c_{M\alpha} = \mathcal{U}\{-2.4,-1.6\}\ [rad^{-1}]$
Constant of tread width tire moment	$\kappa = \mathcal{U}\{-324,-216\}\ [N\,m^2/rad]$

Table 5 Probabilistic robustness validation data

	t_s [sec]	$\lvert\psi_w\rvert_{Max}$ [deg]	$\lvert M_C\rvert_{Max}$ $[Nm]$	ς	$\Im\left[rad^2/s\right]$
Mean	0.017	0.738	1389	0.117	1.34e-5
SD	0.0041	0.017	20	0.053	1.45e-6
Min	0.006	0.691	1329	0.0007	9.97e-6
Max	0.037	0.811	1442	0.413	1.74e-5
$\hat{P}$	0	0	0	0.22	-
L	0	0	0	0.199	-
U	0.0024	0.0024	0.0024	0.242	-

stiffness, $c_{F\alpha}$ and $c_{M\alpha}$, as well as on constant of tread width moment κ are considered because they are related to whether and tire pressure conditions that affect the tire-road interface. In addition, the airplane speed V and the vertical load F_z are considered as varying parameters. Following the work of Barmish and Lagoa (1996), for all of the considered parameters uniform random variation with bounds given in Table 4 was assumed.

To verify the robustness of the proposed controller, 1500 Monte Carlo simulations of the tire damage case were carried out. The probability of violating the criteria, Eq. (14), with the associated 95% confidence intervals [L,U] are given in Table 5 along with the mean and standard deviation values as well as the minimum and maximum values of the investigated quantities. Values for the objective function $\Im$ evaluated over a period of 15 seconds are also listed in Table 5 to compare results with the closed loop data obtained in the nominal case (see Table 3). It appears that the mean, minimum and maximum values of the considered variables taking into account the uniform distribution of the uncertain model parameters match well those of the nominal system.

The obtained results evidenced that the probability of violating the criteria Eq. (14) is null with 95% confidence intervals of L=0.0 and U=0.0024 for the settling time as well as for the maximum absolute values of the fork ration angle and of the control torque. On the other hand, the probability of violating the criterion on the damping ratio, $\varsigma>\varsigma_{\min}$, was 0.22 with 95% confidence bounds L=0.199 and U=*0.242*. The mean value of the damping ratio is 0.117 and matched well with the one obtained in the nominal case. However, the minimum value of ς computed by Eq. (13) was lower than the limit quantity used to define the stochastic robustness verification

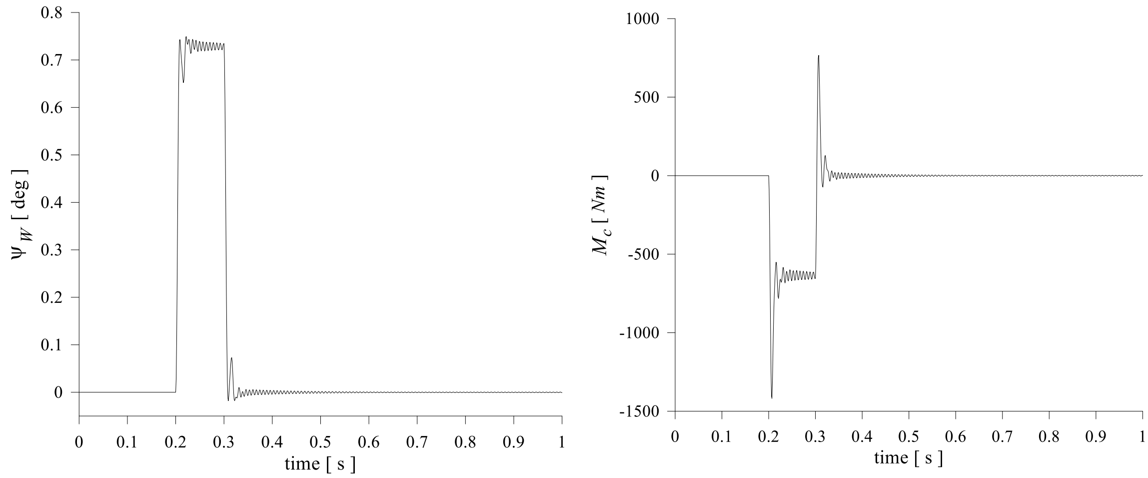

(a) time history of $\psi_W(t)$ (b) time history of $\psi_W(t)$

Fig. 9 Stochastic robustness analysis results: damping ratio worst case.

criterion. With the aim of investigating the system response for the damping ratio worst case, i.e., ς=0.0007, the time history of the fork rotation angle and of the requested control torque are shown in Fig. 9. By looking at the rotation angle time response, it can be noticed that the damping ratio is ς=0.0007 because the first and second minima after the disturbance were almost equal, namely $\psi_{W1}=-0.01803$ deg and $\psi_{W2}=-0.01795$ deg. However in this case the settling time was t_s=0.017 s, the maximum value of the rotation angle was less than 0.8 deg and the maximum absolute value of the control torque demanded by system was less 1.5 kNm. These meant that the criteria on rotation angle, control torque and settling time, see Eq. (14), were met and thus the control system can be considered robust enough even in worst damping ratio case.

4. Conclusions

An active shimmy suppression system has been proposed and analyzed. The active control systems has been assumed to be arranged with an electro-mechanic actuator capable of applying the commanded control torque to the turning tube at the requested frequency. A proportional-integrative-derivative controller with first order filter of derivative was taken into account. The use of the particle swarm optimization method has allowed selecting the optimal parameters of the PID controller based on the minimization of the integral square error objective function. Three different study cases of aeronautical interest have been analyzed. It has been shown that results obtained under open-loop and closed-loop conditions match well with those presented in the literature. Last, in order to verify the robustness of the active control system proposed, the stochastic robustness analysis was used. Four criteria have been defined to analyze the damping capability of the shimmy control system. The stochastic robustness analysis results allowed to verify the robustness of the proposed nonlinear model based active shimmy control system.

References

Ang, K.H., Chong, G. and Li, Y. (2005), "PID control system analysis, design, and technology", *IEEE Tran. Control Syst. Tech.*, **13**(4), 559-576.

Atabay, E. and Ozkol, I. (2014), "Application of a magnetorheological damper modeled using the current-dependent Bouc-Wen model for shimmy suppression in a torsional nose landing gear with and without freeplay", *J. Vib. Control*, **20**(11), 1622-1644.

Barmish, B.R. and Lagoa, C.M. (1997), "The uniform distribution: A rigorous justification for its use in robustness analysis", *Math. Control, Signal. Syst.*, **10**(3), 203-222.

Besselink, I.J.M. (2000), "Shimmy of aircraft main landing gear", Ph.D. Thesis, Delft University of Technology, Delft.

Bonfè, M. (2011), "Discussion on: state feedback fuzzy adaptive control for active shimmy damping", *Eur. J. Control*, **17**(4), 394-396.

European Aviation Safety Agency and Total Training Support Ltd. EASA and TTS (2010), Integrated training system: Module 11A, Volume 5, S.l., TTS Integrated Training System.

Federal Aviation Administration, FAA (2012), AMT Airframe Handbook Volume 2 (FAA-H-8083-31), Aviation Supplies & Academics Inc., Newcastle, WA, U.S.

Howcroft, C., Lowenberg, M., Neild, S., Krauskopf, B. and Coetzee, E. (2014), "Shimmy of an aircraft main landing gear with geometric coupling and mechanical freeplay", *J. Comput. Nonlin. Dyn.*, ASME, **10**(5), 051011.

Huynh, T.H., Pouly, G., Lauffenburger, J.P. and Basset, M. (2008), "Active shimmy damping using direct adaptive fuzzy control", *Proceedings of the 17th IFAC World Congress*, Seul, Korea, July.

Moreland, W.J. (2012), "The story of shimmy", *J. Aeronaut. Sci.*, **21** (12), 793-808.

Pacejka, H. (2005), *Tire and Vehicle Dynamics*, Elsevier, Burlington, MA, USA

Pouly, G., Huynh, T.H., Lauffenburger, J.P. and Basset, M. (2008), "Active shimmy damping using Fuzzy Adaptive output feedback control", *Proceedings of 10th International Conference on Control, Automation, Robotics and Vision, ICARCV 2008*, IEEE, Hanoi, Vietnam, December.

Pouly, G., Huynh, T.H., Lauffenburger, J.P. and Basset, M. (2011), "State feedback fuzzy adaptive control for active shimmy damping", *Eur. J. Control*, **17**(4), 370-393.

Ray, L.R. and Stengel, R.F. (1992), "Stochastic measures of performance robustness in aircraft control systems", *J. Guid. Control Dyn.*, **15**(6), 1381-1387.

Ray, L.R. and Stengel, R.F. (1993), "A Monte Carlo approach to the analysis of control system robustness", *Automatica*, **29**(1), 229-236.

Sateesh, B. and Maiti, D.K. (2009), "Non-linear analysis of a typical nose landing gear model with torsional free play", *Proceedings of the Institution of Mechanical Engineers, Part G: Journal of Aerospace Engineering*, **223**(6), 627-641.

Shi, Y. and Eberhart, R.C. (1999), "Empirical study of particle swarm optimization", *Proceedings of the 1999 Congress on Evolutionary Computation, 1999. CEC 99*, **3**, 1945-1950.

Stépán, G. (2002), "Appell-Gibbs equation for classical wheel shimmy-an energy view", *J. Comput. Appl. Mech.*, **3**(1), 85-92.

Somieski, G. (1997), "Shimmy analysis of a simple aircraft nose landing gear model using different mathematical methods", *Aerosp. Sci. Tech.*, **1**(8), 545-555.

Takács, D., Orosz, G. and Stépán, G. (2009), "Delay effects in shimmy dynamics of wheels with stretched string-like tyres", *Eur. J. Mech. A/Solid.*, **28**(3), 516-525.

Thota, P., Krauskopf, B. and Lowenberg, M. (2009), "Interaction of torsion and lateral bending in aircraft nose landing gear shimmy", *Nonlin. Dyn.*, **57**(3), 455-467.

Von Collani, E. and Dräger, K. (2001), *Binomial Distribution Handbook for Scientists and Engineers*, Springer Science & Business Media.

EC